

Article

Optimization of EPB Shield Performance with Adaptive Neuro-Fuzzy Inference System and Genetic Algorithm

Khalid Elbaz ¹, Shui-Long Shen ^{2,3,4,*}, Annan Zhou ³, Da-Jun Yuan ⁵ and Ye-Shuang Xu ^{1,4,*}

¹ State Key Laboratory of Ocean Engineering, School of Naval Architecture, Ocean, and Civil Engineering, Shanghai Jiao Tong University, Shanghai 200240, China; Khalid@sjtu.edu.cn

² Department of Civil and Environmental Engineering, College of Engineering, Shantou University, Shantou 515063, Guangdong, China

³ Discipline of Civil and Infrastructure, School of Engineering, Royal Melbourne Institute of Technology, Victoria 3001, Australia; annan.zhou@rmit.edu.au

⁴ Department of Civil Engineering, School of Naval Architecture, Ocean, and Civil Engineering, Shanghai Jiao Tong University, Shanghai 200240, China

⁵ School of Civil Engineering, Beijing Jiao Tong University and Tunnel and Underground Engineering Research Center, Ministry of Education, Beijing 100044, China; yuandj603@163.com

* Correspondence: slshen@sjtu.edu.cn or shuilong.shen@rmit.edu.au (S.-L.S.); xuyeshuang@sjtu.edu.cn (Y.-S.X.); Tel.: +86-21-34204301 (S.-L.S.)

Received: 1 February 2019; Accepted: 18 February 2019; Published: 22 February 2019



Abstract: The prediction of earth pressure balance (EPB) shield performance is an essential part of project scheduling and cost estimation of tunneling projects. This paper establishes an efficient multi-objective optimization model to predict the shield performance during the tunneling process. This model integrates the adaptive neuro-fuzzy inference system (ANFIS) with the genetic algorithm (GA). The hybrid model uses shield operational parameters as inputs and computes the advance rate as output. GA enhances the accuracy of ANFIS for runtime parameters tuning by multi-objective fitness function. Prior to modeling, datasets were established, and critical operating parameters were identified through principal component analysis. Then, the tunneling case for Guangzhou metro line number 9 was adopted to verify the applicability of the proposed model. Results were then compared with those of the ANFIS model. The comparison showed that the multi-objective ANFIS-GA model is more successful than the ANFIS model in predicting the advance rate with a high accuracy, which can be used to guide the tunnel performance in the field.

Keywords: advance rate; shield performance; principal component analysis; ANFIS-GA; tunnel

1. Introduction

With the rapid development in many urban areas, tunnel boring machines (TBMs) are frequently used in excavation of long infrastructural tunneling projects. TBMs have become the dominant method of tunneling in many projects such as subways [1–4], railways [5–8], and hydraulic pipelines [9–14]. Therefore, proper estimation of TBM performance is an essential component of tunnel design and for the selection of appropriate excavation machine. Earth pressure balance (EPB) shield machine is a type of TBM that could be adopted in unstable ground [15]. Thus, the accurate prediction model of EPB shield performance could be adopted to solve key problems such as project planning, cost forecast, and optimization of operating parameters.

Over the past few decades, several theoretical and empirical models have been developed for estimating TBM performance [16–26]. Input parameters in these theoretical and empirical models

can be classified into two categories: (1) geological parameters (e.g., intact rock properties, geological strength index, etc.), and (2) operational parameters (e.g., cutter head torque, screw rate, etc.). Due to large complexity in geological conditions and TBM performance prediction, theoretical and empirical models cannot effectively present the dynamic and nonlinear nature of TBM performance. Therefore, artificial intelligence (AI) models can overcome these limitations by using a sufficient amount of field data. These models can create non-linear relationships between inputs and system output. AI models have been widely applied by many researchers in several tunneling projects [27–32]. Typical AI models include artificial neural network (ANN) [33–35], fuzzy logic (FL) model [36], Genetic algorithm (GA) [37,38], and adaptive neuro-fuzzy inference system (ANFIS) [39,40]. Minh et al. [41] developed the fuzzy logic model as an alternative method that was more accurate in comparison with four statistical regression models to predict the TBM performance. Their results indicated that the rock properties can affect the penetration rate of TBM. Salimi et al. [42] illustrated that the ANFIS can be successfully applied to model the nonlinear relation between different parameters involved in the tunneling project. However, AI models still suffer from local minima and poor generalization. Thus, there is a need for prevailing optimization algorithms to overcome such limitations. The genetic algorithm (GA) is an influential population-based technique that able to solve the discrete and enhance the generalization performance of the AI methods. As a result, several hybrid methods have been developed by integrating the optimization algorithms with AI techniques. For instance, Murlidhar et al. [43] developed a hybrid model of GA with ANN for predicting the interlocking of shale rock samples, with better prediction accuracies than the simple ANN technique. However, further developments for AI models are still required. Moreover, the seeking for optimization technique is essential to achieve the best design with minimizing the fitness function by varying design variables while satisfying design constraints. To overcome inaccuracies and uncertainties that exist in conventional models, multi-objective optimization models are more suitable.

In this study, a multi-objective ANFIS-GA model was proposed and applied to predict the EPB shield performance. Principal component analysis (PCA) was performed to examine the effect of various shield parameters on the advance rate of shield machine. In order to assess the performance of the hybrid ANFIS-GA model, its prediction results were compared with those from the ANFIS model. The remainder of this paper is organized as follows. Section 2 describes the structure of the adaptive model. Section 3 analyzes the real field database of shield performance. The simulation results are presented in Section 4. Finally, conclusions are summarized in Section 5.

2. Methodology

2.1. Adaptive Neuro-Fuzzy Inference System (ANFIS)

Fuzzy logic (FL) model is an algorithm that has gained popularity in different engineering fields. The advantages of FL are the ability to make a decision, despite the dominant uncertainty and inaccuracy of several field problems. However, this method does not offer preferable results in unforeseen situations [32]. Many extensions of the fuzzy logic model have been developed to overcome this limitation. Additionally, the ANN technique can adapt its abilities of learning and is effective to model a variety of real applications; however, it still has some limitations. When the input data is subject to a high level of uncertainty or ambiguity, ANFIS techniques perform better [44]. ANFIS is a soft computing technique developed by Jang [44] to solve the complicated and nonlinear issues. This technique combines the fuzzy logic model with adaptive neural networks (ANN) learning technique. ANFIS can analyze and simulate the mapping relation between the input and output dataset over a hybrid system to determine the optimal distribution of membership functions. ANFIS normally involves five layers: fuzzification layer, implication layer, normalization layer, defuzzification layer, and summation layer. These layers comprise several nodes that are defined by the node function. Nodes in each layer have the same function. The network output mainly depends on the adaptable parameters in the nodes. The network learning rules update these parameters in order to minimize

the error. The ANFIS architecture with two inputs and one output is shown in Figure 1. To clarify the structure of ANFIS, two if-then rules based on a Takagi-Sugeno type fuzzy inference system are considered:

$$\text{Rule 1: If } x \text{ is } A_1 \text{ and } y \text{ is } B_1, \text{ then } f_1 = p_1x + q_1y + r_1 \tag{1}$$

$$\text{Rule 2: If } x \text{ is } A_2 \text{ and } y \text{ is } B_2, \text{ then } f_2 = p_2x + q_2y + r_2 \tag{2}$$

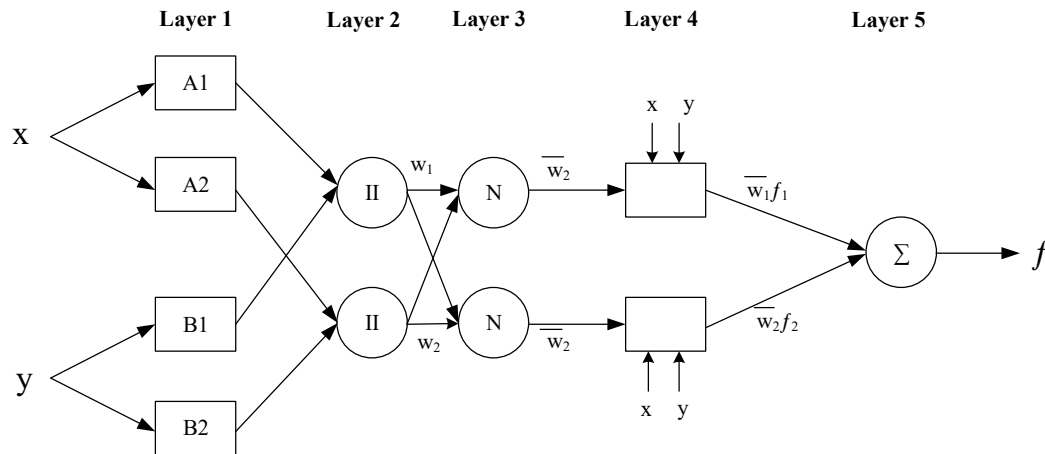


Figure 1. A basic structure of the adaptive neuro-fuzzy inference system (ANFIS) model.

In the expressed rules, $A_{1,2}$ and $B_{1,2}$ are fuzzy sets of input premise parameters x and y ; $p_{1,2}$ $q_{1,2}$, $r_{1,2}$ are the consequent parameters and f is the output of the ANFIS model.

The ANFIS structure consists of five different layers (Figure 1) and each layer is briefly described as follows.

Layer 1: this layer is called fuzzification layer; every node in this layer creates a membership grade of a linguistic variable and the output of each node is estimated as follows:

$$Q_i^1 = \mu_{A_i}(x) = \frac{1}{1 + \left[\left(\frac{x - v_i}{\sigma_i} \right)^2 \right]^{b_i}} \tag{3}$$

where, x is the input value of the node i ; A_i is the linguistic variable associated with this node; σ_i , v_i and b_i are the function parameters. The parameters in this layer are defined as the premise parameters.

Layer 2: this layer is called implication layer; each node in this layer calculates the “firing strength” of each rule by multiplying the incoming signals as follows:

$$Q_i^2 = W_i = \mu_{A_i}(x) \cdot \mu_{B_i}(y), \quad i = 1, 2 \tag{4}$$

Layer 3: this layer is the normalization layer; each node in this layer calculates the ratio of the i^{th} rules firing strength to all rules firing strengths. The outputs of this layer are called normalized firing strengths.

$$Q_i^3 = \bar{w}_i = \frac{w_i}{w_1 + w_2}, \quad i = 1, 2 \tag{5}$$

Layer 4: this layer is the defuzzification layer; each node in this layer is the output operators for each rule:

$$Q_i^4 = \bar{w}_i f_i = \bar{w}_i (p_i x + q_i y + r_i), \quad i = 1, 2 \tag{6}$$

where w_i is the output of layer 3; p_i , q_i , and r_i are the consequent parameters that are confirmed in the training process.

Layer 5: this layer is the summation layer; the single node in this layer is a constant node that computes the overall output as the summation of all input signals:

$$Q_i^5 = \text{overall output} = \sum_i \bar{w}_i f_i = \frac{\sum_i w_i f_i}{\sum_i w_i} \tag{7}$$

A hybrid algorithm combining the least squares approach and the gradient descent method is preferred to adjust the ANFIS training problem.

2.2. Fuzzy C-means Clustering

To extract useful patterns/structures from large datasets, different clustering algorithms have been developed and classified into two categories: distinct clustering and fuzzy clustering. In distinct clustering, such as K-mean clustering, every data element is assigned to exactly one cluster [45]. However, the data elements on the boundary of multiple clusters may not belong to any of the multiple clusters. To overcome the classification uncertainty, fuzzy clustering assigns every data element to multiple clusters by combining every data element with a set of membership levels. With the cluster information, a fuzzy inference system can be produced to model data behaviors with the least number of rules.

Fuzzy C-means (FCM) clustering is a robust fuzzy clustering algorithm, appropriate for clustering overlapped datasets. The degree of a data point in FCM is specified by a membership. The membership assigns a large value for the data element close to the cluster center and a small value for the data element away from the cluster center. FCM partitions a choice of n vector x_i , ($i = 1, 2, \dots, n$) into fuzzy sets and estimates the cluster center in each set by minimizing the objective function.

Firstly, there are n data points $(x_1, x_2, x_3, \dots, x_n)$, with the cluster center c_i , $i = 1, 2, \dots, C$ randomly selected. The membership matrix (U) is estimated using the following equation:

$$\mu_{ij} = \frac{1}{\sum_{k=1}^C \left(\frac{d_{ij}}{d_{kj}}\right)^{\frac{2}{m-1}}} \tag{8}$$

where, $d_{ij} = ||c_i - x_j||$ is the Euclidean distance between the i^{th} cluster center and the j^{th} data point; μ_{ij} is the coefficients in the membership matrix; m is the index of fuzziness; c is the total number of clusters.

Secondly, the objective function can be calculated according to the following equation:

$$J(U, c_1, \dots, c_2) = \sum_{i=1}^c J_i = \sum_{i=1}^c \cdot \sum_{j=1}^n \mu_{ij}^m d_{ij}^2 \tag{9}$$

Finally, a new c fuzzy cluster center C_i ($i = 1, 2, \dots, C$) can be estimated as follows:

$$C_i = \frac{\sum_{j=1}^n \mu_{ij}^m x_j}{\sum_{j=1}^n \mu_{ij}^m} \tag{10}$$

In ANFIS, the fuzzy inference system with initial structure has an obvious effect on the modeling accuracy. Therefore, ANFIS has two limitations: slow computational convergence and potential of being trapped in local minima. To overcome these limitations, the fuzzy inference system needs to be optimized with heuristic optimization techniques, such as Genetic algorithm (GA).

2.3. Genetic Algorithm (GA)

Genetic algorithm is one of the evolutionary algorithms inspired by Darwin's theory of biological evolution theory. GA has been applied for optimizing the parameters of the control system that are difficult to solve by traditional optimization techniques [46]. This algorithm has the ability to search efficiently very large solution spaces because GA uses the probabilistic transition rules instead of the deterministic ones. GA repeatedly modifies a population of individual solutions through generations, by randomly selecting individuals from the current generation as parents to produce the children of the next generation, until the population evolves to an optimal solution. In each generation, a new set of approximation is produced by selecting the best number according to the fitness level and reproduction by operators from the natural genetic population. This process leads to an evolution of members that have been adapted to the environment than the initial members, which are in fact their original parents. GA involves three main stages (population initialization, GA operators, evaluation) and illustrated as follows:

- (a) Initialization: randomly create a population of n chromosomes and evaluate the effectiveness of each chromosome using the fitness function.
- (b) GA operators:
 - (i) Selection: select the best two chromosomes from the population based on its fitness; using the selected chromosomes as parents for producing offspring, new child chromosomes, and the next generation.
 - (ii) Crossover: the parent chromosomes intercross randomly with a certain probability and produce the new child (offspring). If the intersection does not occur, the child will be the same as the two parent chromosomes.
 - (iii) Mutation: this operator is used as a random modification for changing some of the genes inside the chromosomes. By mutation, it is conceivable to adjust the diversity of the population and improve the search capacity to avoid the convergence of the algorithm to local optima.
- (c) Evaluation: in this stage, the fitness function usually presents a specific form of the objective function of the optimization problem.

2.4. Multi-Objective Fitness Function

In contrast to the single-objective optimization method, in multi-objective optimization, the fitness function has to adjust all the objectives, which is done by using different assignment strategies [47]. Among the different strategies, one of the most famous scalarization methods for multi-objective optimization techniques is the weighted-sum approach. The weighted-sum approach is adopted by transforming several objectives function into a single objective by assigning weights. Ismail and Yusof [48] stated that the weighted-sum approach is considered as one of the most common techniques in achieving the optimal weights combination. The optimized technique is proposed by using a multi-objective fitness function. This approach distinguishes with the straight forward fitness formulation and computationally efficient. In this approach, the problem is adapted to a single function $F(x)$ with a scalar objective function as illustrated in the following equation:

$$F(x) = \sum_{i=1}^m w_i f_i(x) = w_1 f_1(x) + w_2 f_2(x) + w_3 f_3(x) \quad (11)$$

where, $x = x_1, x_2, x_3, \dots, x_m$ and $w_i = w_1, w_2, w_3, \dots, w_m$.

The weight (w_i) for every fitness function (f_i) is assigned for evaluating fitness. The appropriate weights from the interval [0; 1] are adapted for all objectives as given below:

$$\sum_{i=1}^m w_i = 1 \quad \text{and} \quad 0 \leq w_i \leq 1 \quad (12)$$

2.5. Integrating ANFIS with GA Model

In ANFIS, every input usually includes several membership functions (MFs) and every MF becomes a maximum somewhere. This process needs to be performed with the experience that the changes in the position of belonging functions can change the prediction accuracy. In order to optimize the position of MFs and increase the ANFIS accuracy through training process, GA is used. The hybrid model is used to determine more accuracy results for nonlinear problems and to improve the prediction of tunneling performance. The data points can be categorized into two parts, the training set and the testing set. The percentage of the training dataset can be used to create the ANFIS structure model, whereas the testing set can be used to evaluate the model's prediction. In the ANFIS model, training began to use the arranged dataset. The training dataset process permits the system to regulate the defined parameters as input or output in the system. The training set ends when the specified conditions to terminate the program are accepted. The premise and consequent parameters of ANFIS model are updated by the genetic algorithm. The premise parameters in the fuzzification layer denote (σ, ν, b) in Equation (3) that belong to Gauss membership functions and the number of these parameters is equal to the sum of the parameters in all MFs. Consequent parameters are the ones that defined in the defuzzification layer (p, q, r) in Equation (6). For training ANFIS with (M) membership functions and (n) inputs, there are M^n fuzzy rules based on Jang [44]. Figure 2 demonstrates the procedures of the hybrid ANFIS-GA. The multi-objective fitness function has been selected as the evaluation criterion of the training result. The dataflow is presented as:

- Step 1. The first step of the dataflow is to prepare the input parameters (cutter head torque, rotational speed of screw rate, cutter head rotation speed). Then, the corresponding output is set (advance rate).
- Step 2. Initializing the Genetic Algorithm. In this step, the population initialization and GA operators are configured.
- Step 3. In ANFIS configuration, the training and testing data are defined. The 80 percent of the input database is used for the model's training and the rest twenty percent is utilized for the model validation.
- Step 4. Define the number of membership functions and rules. The algorithm applies the combination of least-squares and the backpropagation method to train the fuzzy inference system and emulate the established dataset.
- Step 5. Evaluate the objective function. If the optimum criteria have not been achieved, the selection, crossover, and mutation are applied to define the new population that will be evaluated. If the criteria have been met, the solution is obtained.

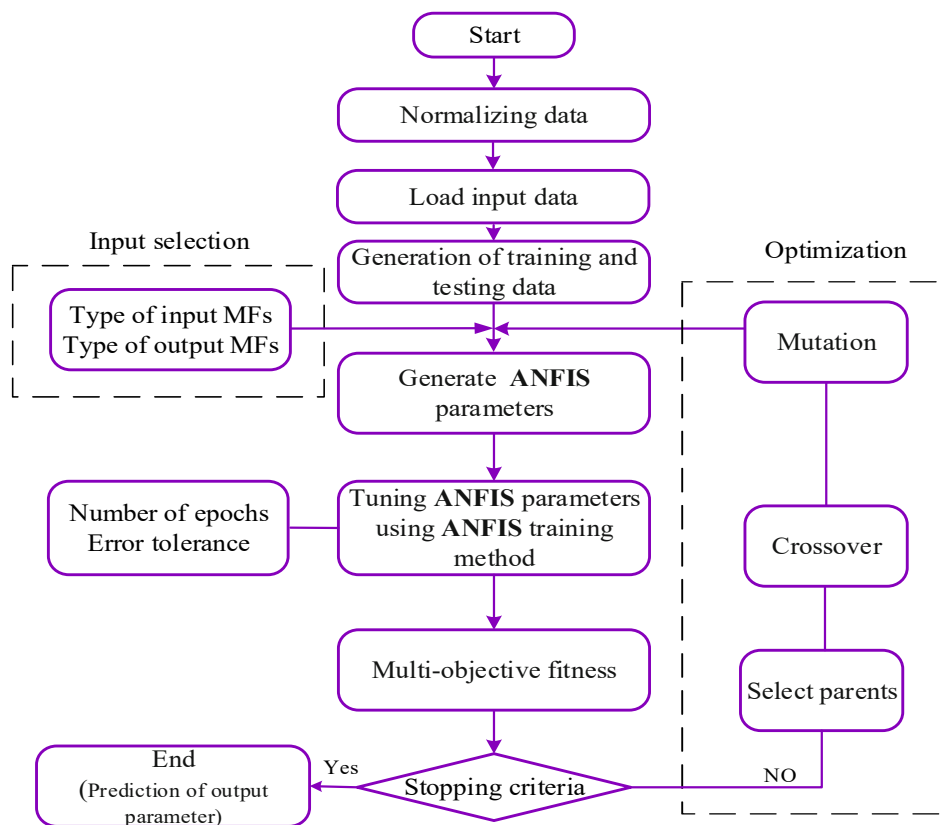


Figure 2. Steps of ANFIS-genetic algorithm (GA) model procedure.

3. Processing Database

3.1. Project Details

In this study, the applicability of the hybrid model through a real field tunnel section in Guangzhou, China was analyzed. This tunnel is located at Ma-Lian section (Huadu area) for Guangzhou Metro Line number 9. The location of the project site is described in Figure 3. An earth pressure balanced TBM of 6.25 m in diameter was used to excavate the tunnel section. The shield machine specifications are summarized in Table 1. The buried depth of the tunnel was varied from 7.0 to 10.0 m. The ring width was 1.6 m and each ring consisted of six segments and one tapered key. The yield strength of the concrete segment (f_c') was 45 MPa. The advancement of shield machine usually encountered a silty clay soil during the tunneling process in the studied section. The geological profile of the encountered soil is displayed in Figure 4. This figure illustrates that the shield machine encountered silty clay soil with water content varying between 25% and 45%. The variation range of void ratio was between 0.7 and 0.85, and the optimum cohesion value was 40 kPa. More information about the tunnel section and the geological conditions can be found in Elbaz et al. [49,50].

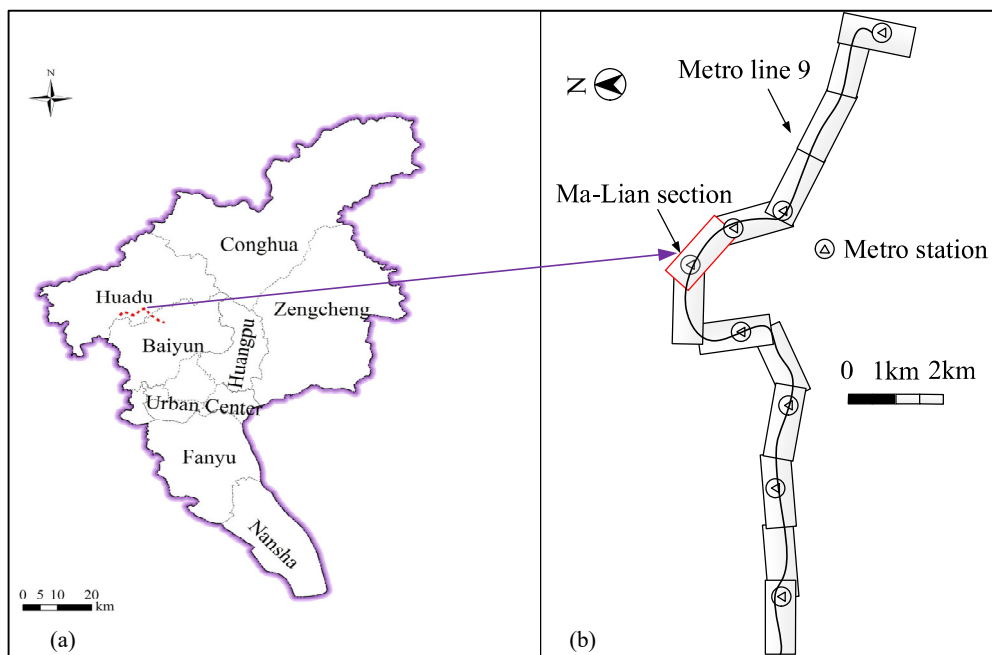


Figure 3. Location of the construction site, (a) map of Guangzhou City, (b) metro line 9.

Table 1. Summary of the main specifications for the earth pressure balance (EPB) shield.

Shield Type	EPB
External diameter (m)	6.25
Inner diameter for lining (m)	5.40
Outer diameter for lining (m)	6.0
Shield length (m)	8.90
Cutterhead power (kW)	600
Number of cutters:	
Disc cutter	40
Scraper	52
Ripper	20
Disc cutter diameter (mm)	432
Shield weight (kN)	Approximately 3000

3.2. Shield Performance Database

All parameters of operational and geological conditions for establishing prediction models in later computations were collected from the testing and monitoring results along the studied section. The shield machine specifications were collected from the documents provided by the manufacturer, as summarized in Table 1. The input shield parameters were extracted directly from a built-in data acquisition system. Among several parameters, preliminary analysis has led to select seven parameters that seem to be the most effective on the advance rate of shield machine [49,51]. These parameters including thrust force (TF), cutter head torque (CT), soil pressure (SP), rotational speed of screw rate (SC), cutter head rotation speed (CR), grouting pressure (GP), burial depth (H), and advance rate (AR). Some basic statistical details of the model inputs and output are illustrated in Table 2. Schematic stages of the present work for the prediction of TBM performance is displayed in Figure 5.

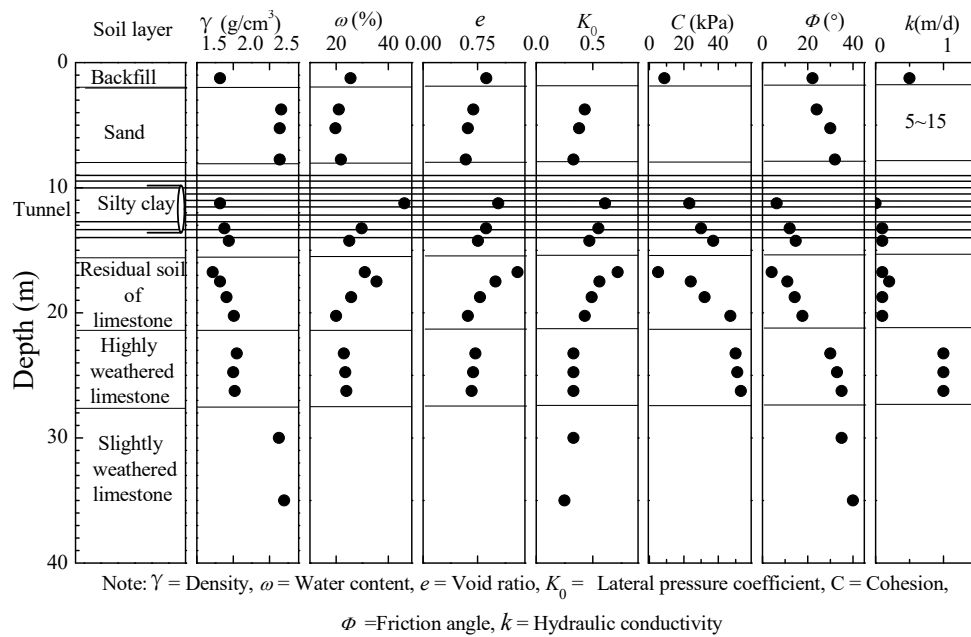


Figure 4. Geotechnical profiles of the construction site.

Table 2. Statistics of the database in this study.

Parameter	Unit	Category	Min.	Max.	Mean
Thrust force (TF)	kN	Input	5600	11,405	8821.18
Cutter head torque (CT)	MN.m	Input	1	4	1.588
Rotational speed of screw rate (SC)	RPM	Input	5	15.5	9.768
Cutter head rotation speed (CR)	RPM	Input	0.9	1.5	1.211
Grouting pressure (GP)	kPa	Input	100	300	188.95
Soil pressure (SP)	kPa	Input	113.33	223.33	151.4
Burial depth (H)	m	Input	7.1	9.38	8.19
Advance rate (AR)	mm/min	Output	20	63	42.25

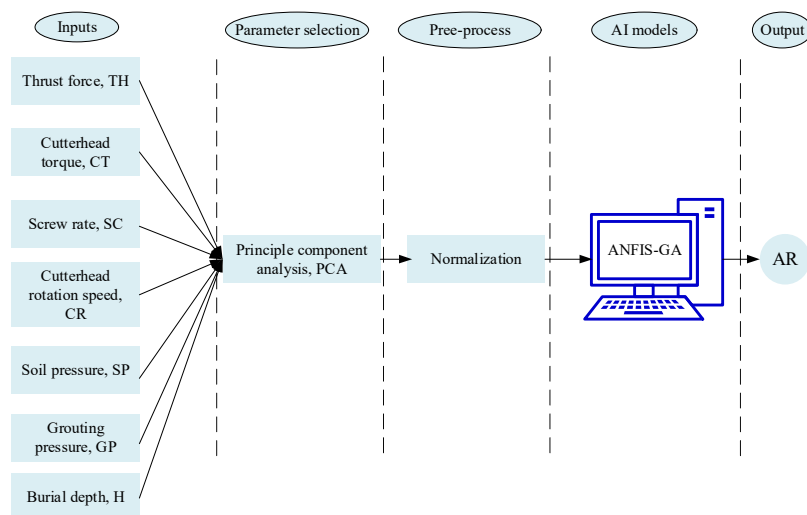


Figure 5. Schematic steps for predicting tunnel boring machines (TBM) performance.

3.3. Principal Component Analysis (PCA)

PCA is a traditional multivariate statistical method that can be utilized to reduce the complex dataset of predictive variables to a lower dimension. PCA provides a few linear combinations of the variables that can be utilized to summarize the data without losing much information during

the analysis. For more information about the structure and implementation of PCA, some other references [39,52] can be considered.

In this study, PCA was performed on a set of input and output parameters and the variance ratio of the first component to the total variance is calculated. Analyses of different parameters were performed to identify the most critical parameters of the shield machine performance. The results of PCA are displayed in Figure 6. It can be seen that the factor containing three input parameters (CT, SC, and CR) is shown to be the most critical parameters, with the greatest variance ratio of 93%. The advance rate of shield machine can be considered as a function of these three inputs. As a result, these three parameters were selected as input parameters for the predictive models.

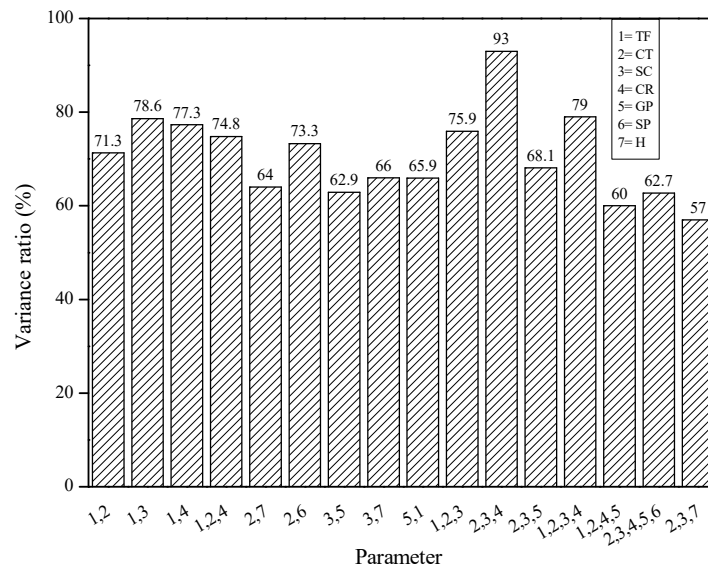


Figure 6. Principal components analysis for some parameters in this study.

4. Results and Discussion

4.1. ANFIS Model

The ANFIS model has been applied to predict the advance rate of shield machine during the tunneling process. To apply this model, three effective parameters (CT, SC, and CR) were set as inputs and AR is set as output. In ANFIS modeling, there are two main stages: the generation of pattern vector and the pattern formation with an input vector and its corresponding target vector. The data range of both input and output is significant and cannot be neglected in different parameters of operating ranges. Thus, all datasets were normalized in the range of (0, 1) to simplify the design procedures using the following equation [53]:

$$X_n = \frac{(X - X_{\min})}{(X_{\max} - X_{\min})} \tag{13}$$

where X and X_n are the measured and normalized values, respectively, and X_{\min} and X_{\max} denote the minimum and maximum values of X , respectively.

In this study, the 200 datasets have been categorized into two subsets randomly. 80% of the whole dataset utilizing to create ANFIS structure are selected as training set and the other 20% utilizing for verifying the models are chosen as testing set, following the recommendation of Swingler [54]. Figure 7 displays the architecture of ANFIS with three input parameters and one output. For ANFIS model, the number and kind of the membership functions (MFs) and epoch number should be provided. As mentioned in the previous literature, there are no explicit methods or formulas to predict the necessary membership functions [55–57]. Thus, the MFs were estimated by way of trial and error. The best estimates were acquired from the Gaussian type (Table 3). The Takagi-Sugeno method was applied because of its higher reliability and computational efficiency for developing a systematic

technique to construct fuzzy rules from the input-output dataset. The initial fuzzy inference system (FIS) was generated using fuzzy c-mean clustering method. MATLAB software was applied with the Genfis3 function to adjust the initial fuzzy inference system of the model. Figure 8 shows the correlation coefficient for the training and testing dataset. This figure illustrates that the relation between the measured and the predicted AR are more applicable in training dataset than in testing dataset.

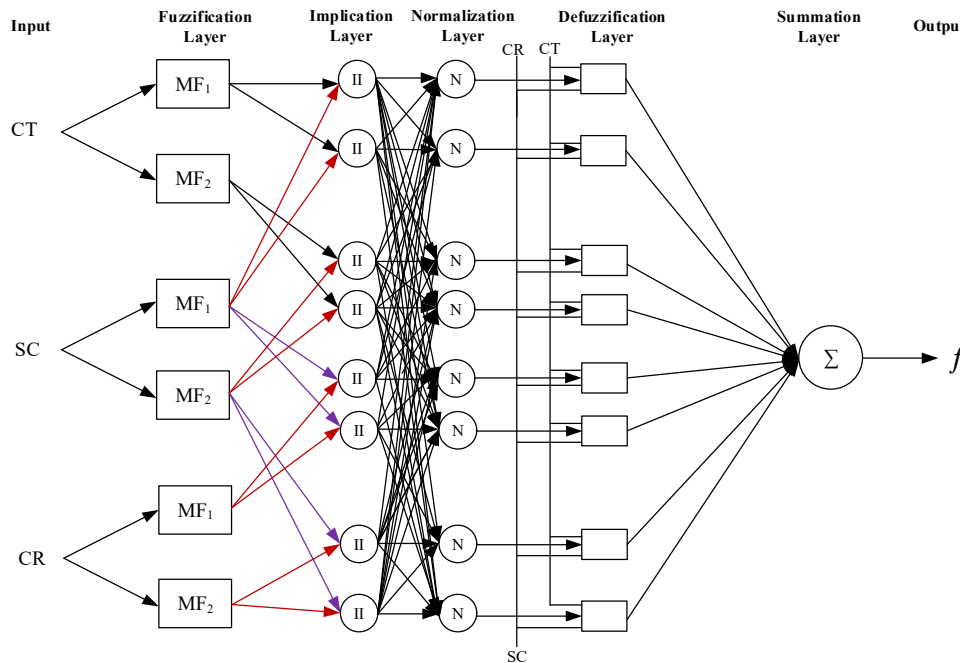


Figure 7. The ANFIS network-based architecture.

Table 3. ANFIS-GA model’s analytical details.

ANFIS Parameter Type	Characteristic/Value
Membership function (MF) type	Gaussian
Fuzzy structure	Takagi-Sugeno-type
Output MF	Linear
Number of fuzzy rules	8
Number of Epoch in ANFIS	200
Minimum Improvement	1×10^{-5}
Type of initial fuzzy inference system	Genfis 3
Initial step size	0.01
Step size decrease rate	0.9
Step size increase rate	1.1
Number of training data pairs	160
Number of testing data pairs	40
Training method	GA
Maximum number of generations	1000

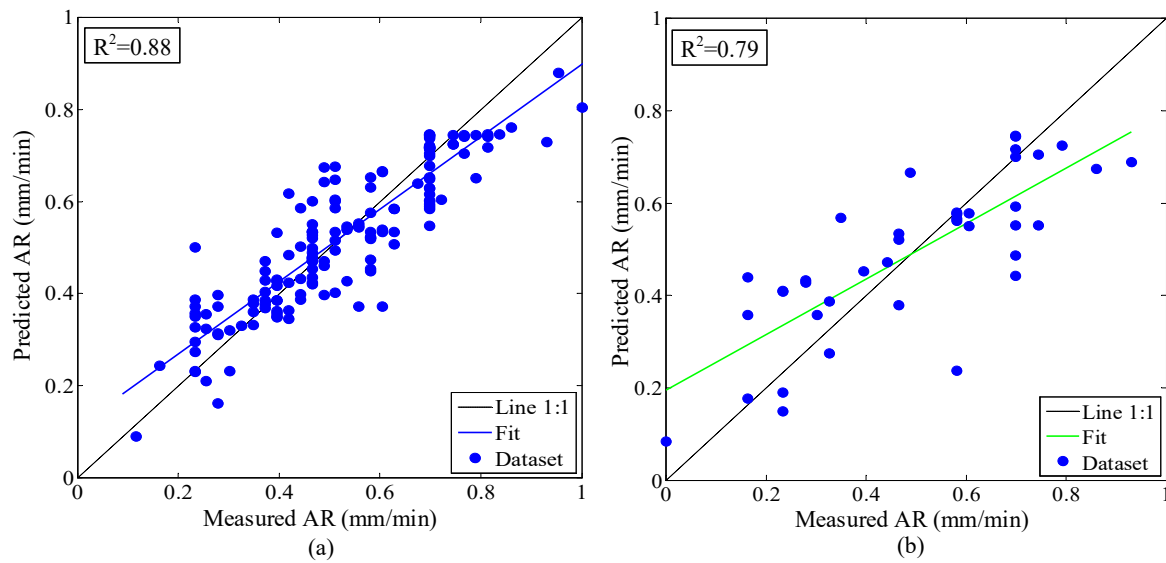


Figure 8. Comparison between measured and predicted AR from ANFIS model: (a) training set and (b) testing set.

4.2. ANFIS-GA Model

To predict the advance rate of shield machine with high accuracy, a hybrid ANFIS-GA was applied in this study. The ANFIS provided the search space and utilized GA for finding the best solution by tuning the membership functions required to reach the lower error. The idea of hybrid technique was proposed to predict the EPB shield performance that creates a non-linear relationship between the input variables and targets to estimate the outputs. As a result, machine performance parameters, such as cutter head torque (CT), rotational speed of screw rate (SC), and cutter head rotation speed (CR), were set as input parameters, and advance rate (AR) was set as the output parameter. The hybrid model was programmed in MATLAB software. ANFIS-GA model was applied in the form of Takagi Sugeno model to integrate the best features of fuzzy inference systems and neural networks. The MFs were considered by Gaussian shapes and the GA parameters were adjusted by the trial and error method. In the study, several attempts were performed to select the various parameter values that are required for GA. As a result of these attempts, population size was selected as 50, crossover rate was chosen as 0.8 and mutation rate was chosen as 0.02. More discussions regarding the hybrid model were presented in Table 3. To evaluate the hybrid model for predicting the advance rate, the multi-objective fitness function is minimized with the following statistical parameters:

$$RMSE = \sqrt{\frac{\sum (x_{mea} - x_{pre})^2}{n}} \tag{14}$$

$$R^2 = 1 - \frac{\sum_{i=1}^n (x_{mea} - x_{pre})^2}{\sum_{i=1}^n (x_{mea} - x_m)^2} \tag{15}$$

$$VA = \left[1 - \frac{\text{var}(x_{mea} - x_{pre})}{\text{var}(x_{mea})} \right] \tag{16}$$

where x_{mea} , x_{pre} , x_m , and n were the measured, predicted, mean of the x values, and the total number of datasets, respectively. Theoretically, a predictive model with high accuracy is desired when root mean square error (RMSE) is equal to 0 and correlation coefficient (R^2) and variance account (VA) are equal to 1.

In the proposed model, the goal of the optimization process was to find the best design variables to maximize correlation coefficient (R^2), variance account (VA), and decrease route mean square error ($RMSE$) at the same time, as displayed in the following Equation:

$$\text{Minimize Fit}(RMSE, R^2, VA) = (-w_1 \times RMSE + w_2 \times R^2 + w_3 \times VA) \tag{17}$$

where $w_1, w_2, w_3 \in (0, 1)$, satisfying $w_1 + w_2 + w_3 = 1$. In this model, the values of w_1, w_2 , and w_3 were determined as 0.8, 0.1, and 0.1, respectively.

Figure 9 shows the relationship between the measured and predicted values acquired from ANFIS-GA predictive model for the training and testing dataset. It can be deduced that the predicted values of AR are less scattered and close to the measured values signified by its closeness to the line of equality (dashed line). To further clarify, the error deviations of outputs of ANFIS-GA model are depicted in Table 4. The relative deviations of the hybrid model were mostly in the range of $\pm 15\%$, demonstrating the more reliability of the proposed model.

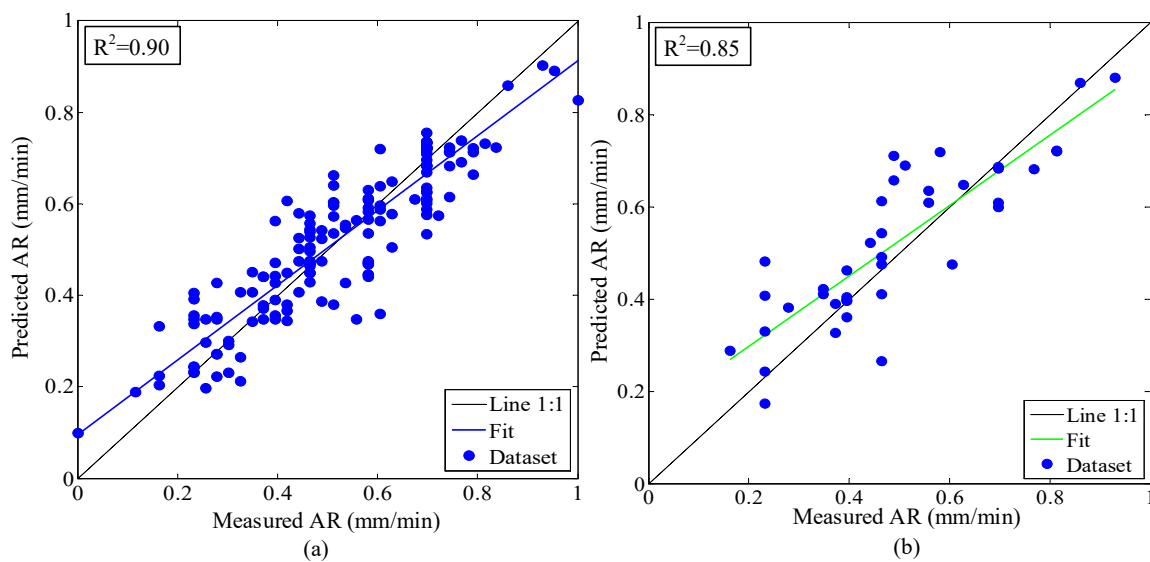


Figure 9. Comparison between measured and predicted AR from the ANFIS-GA model: (a) training set and (b) testing set.

Table 4. The relative deviation of the hybrid ANFIS-GA model.

Model	Number of Data	Relative Deviation
Training data	160	$\pm 15\%$
Testing data	40	$\pm 15\%$

To illustrate the performance of the EPB shield machine during the tunneling process, the values of measured advance rate from field and the predicted values through ANFIS-GA model were plotted for all datasets, as shown in Figure 10. It can be concluded that the measured and predicted data agreed well with each other. Figure 11 shows the assessment results of the hybrid ANFIS-GA compared with ANFIS model. The criterion for the accuracy of hybrid model was the root mean square error ($RMSE$), correlation coefficient (R^2), and Variance account (VA) within the measured and predicted advance rate of the shield machine [58–60]. According to the testing sets, the hybrid ANFIS-GA model had $RMSE = 0.11$, $R^2 = 0.85$, and $VA = 0.77$, while the ANFIS model had $RMSE = 0.15$, $R^2 = 0.79$, and $VA = 0.74$. Because of smaller $RMSE$ and greater values of R^2 and VA , the ANFIS-GA model performed better than the ANFIS model.

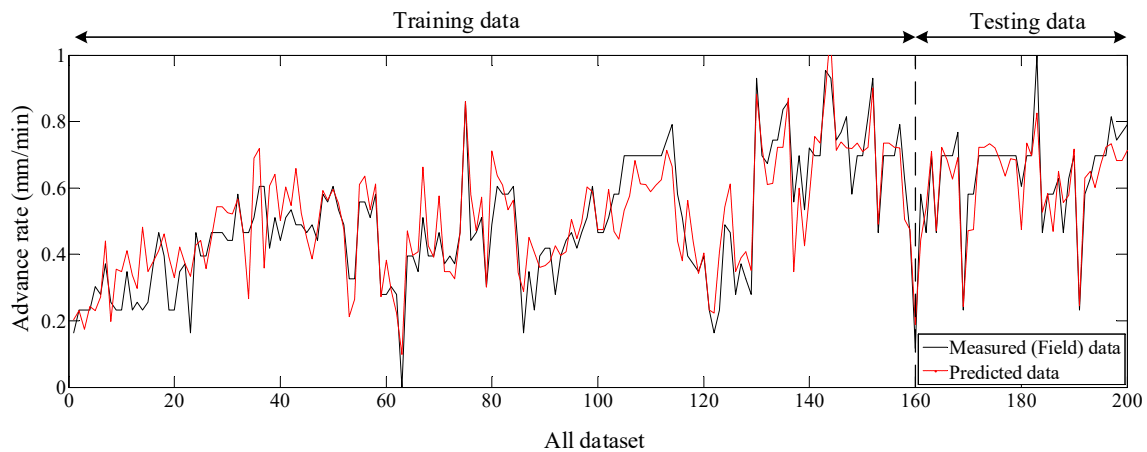


Figure 10. Performance of all measured and predicted database for the ANFIS-GA model.

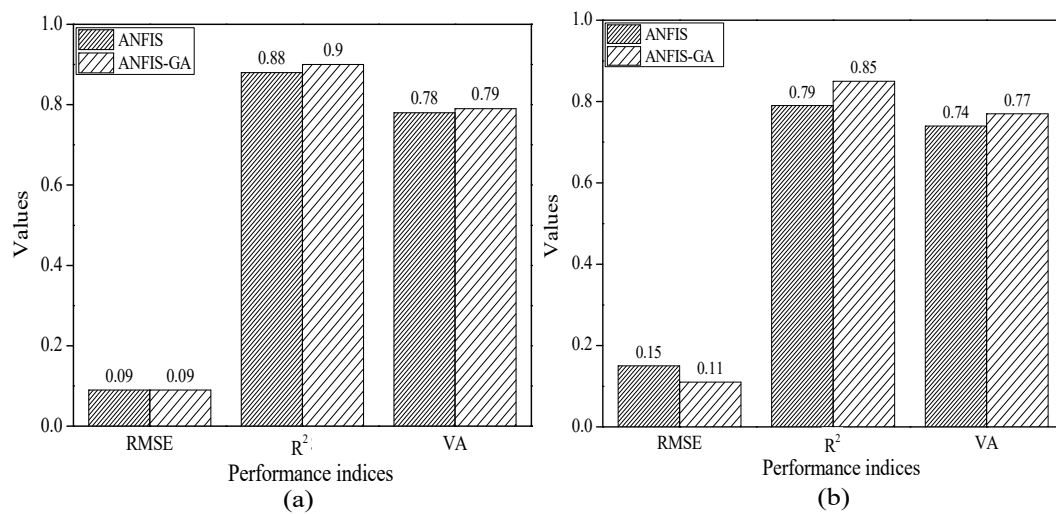


Figure 11. Comparison of performance indices for the ANFIS and the ANFIS-GA: (a) training set and (b) testing set.

5. Conclusions

An effective multi-objective optimization based on integrating adaptive neuro-fuzzy inference system with genetic algorithm was established for predicting the advance rate of the EPB shield machine. The main achievements of this study are outlined as follows:

- (1) Results of principal component statistical analyses illustrated that there was a reasonable relationship between advance rate and three main shield construction parameters including cutterhead torque (CT), rotational speed of screw rate (SC), and cutterhead rotation speed (CR).
- (2) The Multi-objective optimization model was able to successfully predict the shield performance in terms of advance rate, demonstrating a good agreement with the measured field data for both training set and testing set. The ANFIS-GA model showed better prediction accuracy than the ANFIS model.
- (3) The error deviations of the outputs of ANFIS-GA model was in acceptable range $\pm 15\%$, indicating the more reliability of the proposed model in the prediction of advance rate. Therefore, the hybrid model of shield performances can facilitate decision-makers to accurately predict the project duration and the construction cost, thus supporting the development of efficient construction management plans.
- (4) The genetic algorithm was integrated into the process of ANFIS to achieve the optimal solution for ANFIS technique. This was achieved by simultaneously optimizing the ANFIS performance

based on the multi-objective fitness function. The findings illustrated that the hybrid ANFIS–GA provides the promised accuracy with an acceptable interpretation in classification problems. It was difficult to find simpler structures based on satisfactory accuracy and a single optimal algorithm offering the best accuracy for all datasets. However, the algorithm that can lead to a fall balance in accuracy and portability will be more adaptable to real applications. Thus, problems based on this approach are the subject of further work.

Author Contributions: This paper represents a result of collaborative teamwork. Conceptualization, S.-L.S. and K.E.; Methodology, K.E.; Supervision, S.-L.S. and D.-J.Y.; Developed the concept and wrote the manuscript, K.E.; Review and editing, A.Z.; Visualization, A.Z.; Y.-S.X.; Significant comments, Y.-S.X., D.-J.Y. All authors have read and approved the final manuscript.

Funding: The research work described herein was funded by the National Basic Research Program of China (973 Program: 2015CB057806).

Acknowledgments: The research work described herein was funded by the National Basic Research Program of China. This financial support is gratefully acknowledged.

Conflicts of Interest: The authors declare no conflict of interest.

References

1. Liu, X.X.; Shen, S.L.; Xu, Y.S.; Yin, Z.Y. Analytical approach for time-dependent groundwater inflow into shield tunnel face in confined aquifer. *Int. J. Numer. Anal. Methods Geomech.* **2018**, *42*, 655–673. [[CrossRef](#)]
2. Liu, X.X.; Shen, S.L.; Zhou, A.N.; Xu, Y.S. Evaluation of foam conditioning effect on groundwater inflow at tunnel cutting face. *Int. J. Numer. Anal. Methods Geomech.* **2019**, *43*, 463–481. [[CrossRef](#)]
3. Lyu, H.M.; Sun, W.J.; Shen, S.L.; Arulrajah, A. Flood risk assessment in metro systems of mega-cities using a GIS-based modeling approach. *Sci. Total Environ.* **2018**, *626*, 1012–1025. [[CrossRef](#)] [[PubMed](#)]
4. Lyu, H.M.; Shen, S.L.; Zhou, A.N.; Yang, J. Perspectives for flood risk assessment and management for mega-city metro system. *Tunn. Undergr. Space Technol.* **2019**, *84*, 31–44. [[CrossRef](#)]
5. Bilgin, N. An appraisal of TBM performances in Turkey in difficult ground conditions and some recommendations. *Tunn. Undergr. Space Technol.* **2016**, *57*, 265–276. [[CrossRef](#)]
6. Lyu, H.M.; Wang, G.F.; Cheng, W.C.; Shen, S.L. Tornado hazards on June 23rd in Jiangsu Province, China: Preliminary investigation and analysis. *Nat. Hazard* **2017**, *85*, 597–604. [[CrossRef](#)]
7. Lyu, H.M.; Shen, S.L.; Arulrajah, A. Assessment of geohazards and preventive countermeasures using AHP incorporated with GIS in Lanzhou, China. *Sustainability* **2018**, *10*, 304. [[CrossRef](#)]
8. Zhang, Z.; Aqeel, M.; Li, C.; Sun, F. Theoretical prediction of wear of disc cutters in tunnel boring machine and its application. *J. Rock Mech. Geotech. Eng.* **2019**, *11*, 111–120. [[CrossRef](#)]
9. Elbaz, K.; Shen, S.L.; Arulrajah, A.; Horpibulsuk, S. Geohazards induced by anthropic activities of geoconstruction: A review of recent failure cases. *Arab. J. Geosci.* **2016**, *9*, 708. [[CrossRef](#)]
10. Shen, S.L.; Wu, Y.X.; Misra, A. Calculation of head difference at two sides of a cut-off barrier during excavation dewatering. *Comput. Geotech.* **2017**, *91*, 192–202. [[CrossRef](#)]
11. Tan, Y.; Lu, Y. Responses of shallowly buried pipelines to adjacent deep excavations in Shanghai soft ground. *J. Pipeline Syst. Eng. Pract.* **2018**, *9*, 05018002. [[CrossRef](#)]
12. Xu, Y.S.; Shen, S.L.; Lai, Y.; Zhou, A.N. Design of Sponge City: Lessons learnt from an ancient drainage system in Ganzhou, China. *J. Hydrol.* **2018**, *563*, 900–908. [[CrossRef](#)]
13. Xu, Y.S.; Shen, J.S.; Wu, H.N.; Zhang, N. Risk and impacts on the environment of free-phase biogas in Quaternary deposits along the coastal region of Shanghai. *Ocean Eng.* **2017**, *137*, 129–137. [[CrossRef](#)]
14. Xu, Y.S.; Shen, S.L.; Ma, L.; Sun, W.J.; Yin, Z.Y. Evaluation of the blocking effect of retaining walls on groundwater seepage in aquifers with different insertion depths. *Eng. Geol.* **2014**, *183*, 254–264. [[CrossRef](#)]
15. Wu, Y.X.; Shen, J.S.; Cheng, W.C.; Hino, T. Semi-analytical solution to pumping test data with barrier, wellbore storage, and partial penetration effects. *Eng. Geol.* **2017**, *226*, 44–51. [[CrossRef](#)]
16. Shen, S.L.; Wu, H.N.; Cui, Y.J.; Yin, Z.Y. Long-term settlement behavior of metro tunnels in the soft deposits of Shanghai. *Tunn. Undergr. Space Technol.* **2014**, *40*, 309–323. [[CrossRef](#)]
17. Shen, S.L.; Cui, Q.L.; Ho, C.E.; Xu, Y.S. Ground response to multiple parallel microtunneling operations in cemented silty clay and sand. *J. Geotech. Geoenviron. Eng.* **2016**, *142*, 04016001. [[CrossRef](#)]

18. Wu, H.N.; Shen, S.L.; Liao, S.M.; Yin, Z.Y. Longitudinal structural modelling of shield tunnels considering shearing dislocation between segmental rings. *Tunn. Undergr. Space Technol.* **2015**, *50*, 317–323. [[CrossRef](#)]
19. Wu, Y.X.; Shen, S.L.; Yuan, D.J. Characteristics of dewatering induced drawdown curve under blocking effect of retaining wall in aquifer. *J. Hydrol.* **2016**, *539*, 554–566. [[CrossRef](#)]
20. Rostami, J. Performance prediction of hard rock tunnel boring machines (TBMs) in difficult grounds. *Tunn. Undergr. Space Technol.* **2016**, *56*, 173–182. [[CrossRef](#)]
21. Khandelwal, M.; Shirani, R.; Masoud, F. Function development for appraising brittleness of intact rocks using genetic programming and non-linear multiple regression models. *Eng. Comput.* **2017**, *33*, 13–21. [[CrossRef](#)]
22. Xie, X.; Wang, Q.; Huang, Z. Parametric analysis of mixshield tunnelling in mixed ground containing mudstone and protection of adjacent buildings: Case study in Nanning metro containing mudstone and protection of adjacent buildings. *Eur. J. Environ. Civ. Eng.* **2017**, *22*, s130–s148. [[CrossRef](#)]
23. Salimi, A.; Rostami, J.; Moormann, C. Evaluating the Suitability of Existing Rock Mass Classification Systems for TBM Performance Prediction by using a Regression Tree. *Procedia Eng.* **2017**, *191*, 299–309. [[CrossRef](#)]
24. Amoun, S.; Sharifzadeh, M.; Shahriar, K.; Rostami, J.; Tarigh, S. Evaluation of tool wear in EPB tunnelling of Tehran Metro, Line 7 Expansion. *Tunn. Undergr. Space Technol.* **2017**, *61*, 233–246. [[CrossRef](#)]
25. Ren, D.J.; Shen, S.L.; Arulrajah, A.; Wu, H.N. Evaluation of ground loss ratio with moving trajectories induced in double-O-tube (DOT) tunnelling. *Can. Geotech. J.* **2018**, *55*, 894–902. [[CrossRef](#)]
26. Wu, Y.X.; Lyu, H.M.; Han, J.; Shen, S.L. Case study: Dewatering-induced building settlement around a deep excavation in the soft deposit of Tianjin, China. *J. Geotech. Geoenviron. Eng. ASCE* **2019**. [[CrossRef](#)]
27. Salimi, A.; Faradonbeh, R.S.; Monjezi, M.; Moormann, C. TBM performance estimation using a classification and regression tree (CART) technique. *Bull. Eng. Geol. Environ.* **2016**, *77*, 429–440. [[CrossRef](#)]
28. Hasanipanah, M.; Shahnazar, A.; Arab, H.; Golzar, S.B.; Amiri, M. Developing a new hybrid-AI model to predict blast-induced Backbreak. *Eng. Comput.* **2017**, *33*, 349–359. [[CrossRef](#)]
29. Jahed Armaghani, D.; Tonnizam, E.; Sundaram, M.; Narita, N.; Yagiz, S. Development of hybrid intelligent models for predicting TBM penetration rate in hard rock condition. *Tunn. Undergr. Space Technol.* **2017**, *63*, 29–43. [[CrossRef](#)]
30. Yin, Z.Y.; Jin, Y.F.; Shen, J.S.; Hicher, P.Y. Optimization techniques for identifying soil parameters in geotechnical engineering: Comparative study and enhancement. *Int. J. Numer. Anal. Methods Geomech.* **2018**, *42*, 70–94. [[CrossRef](#)]
31. Yin, Z.Y.; Wu, Z.Y.; Hicher, P.Y. Modeling the monotonic and cyclic behavior of granular materials by an exponential constitutive function. *J. Eng. Mech. ASCE* **2018**, *144*, 04018014. [[CrossRef](#)]
32. Rini, D.P.; Shamsuddin, S.M.; Yuhaniz, S.S. Particle swarm optimization for ANFIS interpretability and accuracy. *Soft Comput.* **2016**, *20*, 251–262. [[CrossRef](#)]
33. Kahraman, S. Estimating the penetration rate in diamond drilling in laboratory works using the regression and artificial neural network analysis. *Neural Process Lett.* **2016**, *43*, 523–535. [[CrossRef](#)]
34. Ocak, I.; Evren, S.; Rostami, J. Performance prediction of impact hammer using ensemble machine learning techniques. *Tunn. Undergr. Space Technol.* **2018**, *80*, 269–276. [[CrossRef](#)]
35. Stypulkowski, J.B.; Bernardeau, F.G.; Jakubowski, J. Descriptive statistical analysis of TBM performance at Abu Hamour Tunnel Phase I. *Arab. J. Geosci.* **2018**, *11*, 191. [[CrossRef](#)]
36. Acaroglu, O. Prediction of thrust and torque requirements of TBMs with fuzzy logic models. *Tunn. Undergr. Space Technol.* **2011**, *26*, 267–275. [[CrossRef](#)]
37. Liu, K.; Liu, B. Optimization of smooth blasting parameters for mountain tunnel construction with specified control indices based on a GA and ISVR coupling algorithm. *Tunn. Undergr. Space Technol.* **2017**, *70*, 363–374. [[CrossRef](#)]
38. Babak, S.; Anemangely, M.; Sabah, M. Application of hybrid artificial neural networks for predicting rate of penetration (ROP): A case study from Marun oil field. *J. Pet. Sci. Eng.* **2019**, *175*, 604–623.
39. Bouayad, D.; Emeriault, F. Modeling the relationship between ground surface settlements induced by shield tunneling and the operational and geological parameters based on the hybrid PCA/ANFIS method. *Tunn. Undergr. Space Technol.* **2017**, *68*, 142–152. [[CrossRef](#)]
40. Mottahedi, A.; Sereshki, F.; Ataei, M. Development of over break prediction models in drill and blast tunneling using soft computing methods. *Eng. Comput.* **2017**, *34*, 45–58. [[CrossRef](#)]
41. Minh, V.T.; Katushin, D.; Antonov, M.; Veinthal, R. Regression Models and Fuzzy Logic Prediction of TBM Penetration Rate. *Open Eng.* **2017**, *7*, 60–68. [[CrossRef](#)]

42. Salimi, A.; Rostami, J.; Moormann, C.; Delisio, A. Application of non-linear regression analysis and artificial intelligence algorithms for performance prediction of hard rock TBMs. *Tunn. Undergr. Space Technol.* **2016**, *58*, 236–246. [[CrossRef](#)]
43. Murlidhar, B.R.; Ahmed, M.; Mavaluru, D.; Siddiqi, A.F.; Mohamad, E.T. Prediction of rock interlocking by developing two hybrid models based on GA and fuzzy system. *Eng. Comput.* **2018**. [[CrossRef](#)]
44. Jang, J.S.R. ANFIS: Adaptive-network-based fuzzy inference systems. *IEEE Trans. Syst. Man Cybern.* **1993**, *23*, 665–685. [[CrossRef](#)]
45. Suganya, R.; Shanthi, R. Fuzzy C-means algorithm—A review. *Int. J. Sci. Res. Publ.* **2012**, *2*, 1–3.
46. Jalalkamali, A. Using of hybrid fuzzy models to predict spatiotemporal groundwater quality parameters. *Earth Sci. Inf.* **2015**, *8*, 885–894. [[CrossRef](#)]
47. Papon, A.; Riou, Y.; Dano, C.; Hicher, P.Y. Single-and multi-objective genetic algorithm optimization for identifying soil parameters. *Int. J. Numer. Anal. Methods Geomech.* **2012**, *36*, 597–618. [[CrossRef](#)]
48. Ismail, F.S.; Yusof, R. A new self organizing multi-objective optimization method. In Proceedings of the IEEE International Conference on Systems Man & Cybernetics, Istanbul, Turkey, 10–13 October 2010; pp. 1016–1021.
49. Elbaz, K.; Shen, S.L.; Cheng, W.C.; Arulrajah, A. Cutter-disc consumption during earth-pressure-balance tunnelling in mixed strata. *Proc. Inst. Civ. Eng. Geotech. Eng.* **2018**, *171*, 363–376. [[CrossRef](#)]
50. Elbaz, K.; Shen, S.L.; Tan, Y.; Cheng, W.C. Investigation into performance of deep excavation in sand covered karst: A case report. *Soils Found.* **2018**, *58*, 1042–1058. [[CrossRef](#)]
51. Ren, D.J.; Shen, S.L.; Arulrajah, A.; Cheng, W.C. Prediction model of TBM disc cutter wear during tunnelling in heterogeneous ground. *Rock Mech. Rock Eng.* **2018**, *51*, 3599–3611. [[CrossRef](#)]
52. Salimi, A.; Rostami, J.; Moormann, C.; Hassanpour, J. Examining Feasibility of Developing a Rock Mass Classification for Hard Rock TBM Application Using Non-linear Regression, Regression Tree and Generic Programming. *Geotech. Geol. Eng.* **2018**, *36*, 1145–1159. [[CrossRef](#)]
53. Khamesi, H.; Torabi, S.; Mirzaei-Nasirabad, H.; Ghadiri, Z. Improving the performance of intelligent back analysis for tunneling using optimized fuzzy systems: Case study of the Karaj Subway Line 2 in Iran. *J. Comput. Civ. Eng.* **2015**, *29*, 05014010. [[CrossRef](#)]
54. Swingler, K. *Applying Neural Networks: A Practical Guide*; Academic: New York, NY, USA, 1996; p. 442.
55. Rezakazemi, M.; Ghafarinazari, A.; Shirazian, S.; Khoshsima, A. Numerical modeling and optimization of wastewater treatment using porous polymeric membranes. *Polym. Eng. Sci.* **2013**, *53*, 1272–1278. [[CrossRef](#)]
56. Jin, Y.F.; Yin, Z.Y.; Zhou, W.H.; Huang, H.W. Engineering Applications of Artificial Intelligence Multi-objective optimization-based updating of predictions during excavation. *Eng. Appl. Artif. Intell.* **2019**, *78*, 102–123. [[CrossRef](#)]
57. Cheng, W.C.; Ni, J.C.; Shen, S.L. Experimental and analytical modeling of shield segment under cyclic loading. *Int. J. Geomech. ASCE* **2017**, *17*, 04016146. [[CrossRef](#)]
58. Zeng, C.F.; Zheng, G.; Xue, X.L.; Mei, G.X. Combined recharge: A method to prevent ground settlement induced by redevelopment of recharge wells. *J. Hydrol.* **2019**, *568*, 1–11. [[CrossRef](#)]
59. Xu, Y.S.; Shen, S.L.; Ren, D.J.; Wu, H.N. Analysis of factors in land subsidence in Shanghai: A view based on Strategic Environmental Assessment. *Sustainability* **2016**, *8*, 573. [[CrossRef](#)]
60. Zeng, C.F.; Xue, X.L.; Zheng, G.; Xue, T.Y.; Mei, G.X. Responses of retaining wall and surrounding ground to pre-excavation dewatering in an alternated multi-aquifer-aquitard system. *J. Hydrol.* **2018**, *559*, 609–626. [[CrossRef](#)]

